# Crystal, Molecular, and Electronic Structures of Pentaammineruthenium(III)-Thioether Complexes

**Karsten Krogh-Jespersen,* Xiaohua Zhang, John D. Westbrook, Ronald Fikar, Kasinath Nayak, Whei-Lu Kwik,[1] Joseph A. Potenza,* and Harvey J. Schugar***

*Contribution from the Department of Chemistry, Rutgers, The State University of New Jersey, New Brunswick, New Jersey 08903.* *Received August 8, 1988*

**Abstract:** The nature of Ru(III)-thioether bonding has been probed by a combination of structural, spectroscopic, and molecular orbital methods. The first structural studies of pentaammineruthenium(III)L complexes (L = tetrahydrothiophene, methyl ethyl thioether, and dimethyl thioether) are presented. Crystals of $(NH_3)_5RuSC_4H_8 \cdot 1.5S_2O_6 \cdot 3H_2O$ are triclinic, space group $P\bar{1}$, with $a$ = 10.3622 (6) Å, $b$ = 13.3864 (4) Å, $c$ = 8.2345 (5) Å, $\alpha$ = 98.135 (4)°, $\beta$ = 113.602 (5)°, $\gamma$ = 98.773 (4)°, $V$ = 1008.2 (2) Å$^3$, $Z$ = 2, $R_F$ ($R_{wF}$) = 0.028 (0.044) for 3436 reflections. Crystals of $(NH_3)_5RuSC_3H_8 \cdot 1.5PF_6 \cdot 1.5F$ are triclinic, space group $P\bar{1}$, with $a$ = 10.1911 (8) Å, $b$ = 11.5361 (9) Å, $c$ = 8.2431 (5) Å, $\alpha$ = 109.056 (5)°, $\beta$ = 97.696 (6)°, $\gamma$ = 73.237 (7)°, $V$ = 876.2 (2) Å$^3$, $Z$ = 2, $R_F$ ($R_{wF}$) = 0.029 (0.052) for 3366 reflections. Crystals of $(NH_3)_5RuSC_2H_6 \cdot 2Cl \cdot PF_6$ are orthorhombic, space group $Imm2$, with $a$ = 7.780 (2) Å, $b$ = 10.971 (1) Å, $c$ = 8.936 (1) Å, $V$ = 762.7 (3) Å$^3$, $Z$ = 2, $R_F$ ($R_{wF}$) = 0.035 (0.047) for 818 reflections. The structures consist of $(NH_3)_5Ru^{III}L$ cations separated by the various anions and, in one case, lattice water molecules. The cations exhibit distorted octahedral coordination geometries; Ru-N and Ru-S bond distances span the ranges 2.097 (2)-2.126 (2) and 2.3666 (7)-2.384 (2) Å, respectively. Combined steric and electronic effects serve to tilt the $SC_2$ planes away from the cis ammine groups. Crystals of the dimethyl thioether derivative are twinned. Ab initio molecular orbital calculations were performed on the $(NH_3)_5Ru^{III}$-dimethyl thioether complex with the use of effective core potentials for the inner atomic electrons and extended valence basis sets. Geometry optimization yields good agreement between calculated and experimental structures. The interactions between the high-lying thioether donor orbitals and the Ru(III) 4d orbitals are discussed in detail and the factors determining the unusual thioether coordination geometry are elucidated. Electronic population analysis of the dimethyl thioether complex indicates that the Ru atom carries a positive charge of 0.90e, reduced from the formal triple charge by donation of 0.43e from the thioether ligand and an average of 0.33e from each ammine group. Excited-state calculations with the INDO/S semiempirical MO method on the $(NH_3)_5Ru^{III}$(tetrahydrothiophene) chromophore allow the four observed electronic absorptions in the 20000-50000-cm$^{-1}$ region to be assigned. Two of these are S → Ru(III) charge-transfer absorptions to the half-filled Ru $d_{xy}$ orbital. A third is to the empty $d_{x^2-y^2}$ orbital which is lowered in energy owing to the surprisingly weak thioether ligand field associated with the peculiar mode of thioether bonding.

The molecular and electronic structures of pentaammineruthenium(II,III)L chromophores (L = imidazole, thioether) are relevant to their use in studies of long-range electron transfer. We have reported elsewhere[2,3] on the molecular and electronic structures of the $(NH_3)_5Ru^{III}$-imidazole chromophore whose use as an electron-transfer probe in modified cytochrome $c$,[4,5] azurin,[6] and myoglobin[7] has been a subject of considerable current interest. Although the substantial kinetic stability[8] of $(NH_3)_5Ru^{II,III}$-thioether complexes might be exploited to produce derivatized metalloproteins having one or more $(NH_3)_5Ru$ probes attached to methionine thioether groups, this application does not appear to have been realized yet. However, another feature of Ru(II,-III)-thioether chromophores has considerable promise for revealing important features of long-range electron transfer in nonbiological model systems. This pertains to the details of electronic coupling between electron donors and acceptors separated by a rigid hydrocarbon spacer. If the spacer is an oligospirocyclobutane whose termini are thietanes, it is possible to attach a $(NH_3)_5Ru^{II}$ unit to one end and a $(NH_3)_5Ru^{III}$ unit to the other end. The Ru(II) → Ru(III) metal-metal charge-transfer process results in an "intervalence" absorption that appears in the near-IR spectral region.[9,10] The energy of the intervalence absorption depends upon (among other factors) the reorganization of the metal coordination spheres and solvent shells that accompany electron transfer. An estimate of the electronic coupling between the Ru(II) donor and the Ru(III) acceptor may be obtained from the measured intensity of the intervalence absorption using the Marcus/Hush[11] or Hopfield[12] theories.

Structural data for monomeric reference $(NH_3)_5Ru^{II}$-thioether and $(NH_3)_5Ru^{III}$-thioether complexes are required to predict the energy for metal coordination sphere reorganization that accompanies the above intervalence absorption and to establish precise molecular geometries for future calculations on such systems. A second point of interest concerns the surprisingly low oscillator strength ($\epsilon$ = ca. 100) of the thioether → Ru(III) ligand to metal charge-transfer (LMCT) absorption exhibited by $(NH_3)_5Ru^{III}$-thioether systems.[13] This absorption is a factor of ~30 weaker than the corresponding absorption of Cu(II)-thioether complexes.[14]

We report here X-ray structural and electronic spectroscopic studies of three $(NH_3)_5Ru^{III}L$ complexes (L = tetrahydrothiophene, methylethylthioether, and dimethylthioether). The ground-state electronic structure of the $(NH_3)_5Ru^{III}$-dimethyl thioether system has been examined by ab initio molecular orbital methods and the electronically excited states of the tetrahydro-

(1) Permanent address: National University of Singapore, Kent Ridge, Singapore.
(2) Krogh-Jespersen, K.; Westbrook, J. D.; Potenza, J. A.; Schugar, H. J. *J. Am. Chem. Soc.* **1987**, *109*, 7025.
(3) Krogh-Jespersen, K.; Schugar, H. J. *Inorg. Chem.* **1984**, *23*, 4390.
(4) (a) Isied, S. S.; Kuehn, C.; Worosila, G. J. *J. Am. Chem. Soc.* **1984**, *106*, 1722. (b) Bechtold, R.; Kuehn, C.; Lepre, C.; Isied, S. S. *Nature (London)* **1986**, *322*, 286.
(5) Nocera, D. G.; Winkler, J. R.; Yocom, K. M.; Bordignon, E.; Gray, H. B. *J. Am. Chem. Soc.* **1984**, *106*, 5145.
(6) (a) Margalit, R.; Kostic, N. M.; Che, C.-M.; Blair, D. F.; Chiang, H.-J.; Pecht, I.; Shelton, J. B.; Shelton, J. R.; Schroeder, W. A.; Gray, H. B. *Proc. Natl. Acad. Sci. U.S.A.* **1984**, *81*, 6554. (b) Kostic, N. M.; Margalit, R.; Che, C.-M.; Gray, H. B. *J. Am. Chem. Soc.* **1983**, *105*, 7765. (c) Gray, H. B. *Chem. Soc. Rev.* **1986**, *15*, 17.
(7) (a) Crutchley, R. J.; Ellis, W. R., Jr.; Gray, H. B. *J. Am. Chem. Soc.* **1985**, *107*, 5002. (b) Axup, A. W.; Albin, M.; Mayo, S. L.; Crutchley, R. J.; Gray, H. B. *J. Am. Chem. Soc.* **1988**, *110*, 435. (c) Karas, J. L.; Lieber, C. M.; Gray, H. B. *J. Am. Chem. Soc.* **1988**, *110*, 599.
(8) Kuehn, C. G.; Taube, H. *J. Am. Chem. Soc.* **1976**, *98*, 689.
(9) Stein, C. A.; Taube, H. *J. Am. Chem. Soc.* **1981**, *103*, 693.
(10) Stein, C. A.; Lewis, N. A.; Seitz, G. *J. Am. Chem. Soc.* **1982**, *104*, 2596.
(11) Meyer, T. J. In *Progress in Inorganic Chemistry*; Lippard, S. J., Ed.; John Wiley & Sons, Inc.: New York, 1983; Vol. 30, p 389.
(12) Beratan, D. N.; Hopfield, J. J. *J. Am. Chem. Soc.* **1984**, *106*, 1584.
(13) Stein, C. A.; Taube, H. *J. Am. Chem. Soc.* **1978**, *100*, 1635.
(14) Dagdigian, J. V.; McKee, V.; Reed, C. A. *Inorg. Chem.* **1982**, *21*, 1332, and references cited therein.

0002-7863/89/1511-4082$01.50/0 

Table I. Crystal and Refinement Data for 1–3

| | 1 | 2 | 3 |
|---|---|---|---|
| formula | $RuS_4O_{12}N_5C_4H_{29}$ | $Ru_2S_2P_3F_{21}N_{10}C_6H_{46}$ | $RuCl_2SPF_6N_5C_2H_{21}$ |
| fw | 568.63 | 1016.66 | 464.24 |
| $a$, Å | 10.3622 (6) | 10.1911 (8) | 7.780 (2) |
| $b$, Å | 13.3864 (4) | 11.5361 (9) | 10.971 (1) |
| $c$, Å | 8.2345 (5) | 8.2431 (5) | 8.936 (1) |
| $\alpha$, deg | 98.135 (4) | 109.056 (5) | 90 |
| $\beta$, deg | 113.602 (5) | 97.696 (6) | 90 |
| $\gamma$, deg | 98.773 (4) | 73.237 (7) | 90 |
| $V$, Å$^3$ | 1008.2 (2) | 876.2 (2) | 762.7 (3) |
| $Z$ | 2 | 1 | 2 |
| space group | $P\bar{1}$ | $P\bar{1}$ | $Imm2$ |
| no. ref used to detn cell const | 25 | 25 | 25 |
| $d_{calcd}$, g/cm$^3$ | 1.873 | 1.927 | 2.02 |
| $d_{obsd}$, g/cm$^3$ | 1.87 (1) | 1.93 (1) | 1.98 (2) |
| radiation used | graph. mono. Mo K$\alpha$ (0.71073 Å) | | |
| linear abs coeff, cm$^{-1}$ | 12.2 | 12.2 | 16.5 |
| cryst dimensns, mm | 0.23 × 0.45 × 0.09 | 0.23 × 0.35 × 0.04 | 0.43 × 0.13 × 0.06 |
| rel trans factor range | 0.94–1.00 | 0.96–1.00 | 0.91–1.00 |
| diffractometer | Enraf-Nonius CAD-4 | | |
| data collctn method | $\theta$–$2\theta$ | | |
| $2\theta$ range, deg | 4–52 | 4–52 | 4–60 |
| temp, K | 296 (1) | 297 (1) | 296 (1) |
| scan range, deg | 0.7 + 0.3 tan $\theta$ | 0.7 + 0.3 tan $\theta$ | 0.9 + 0.35 tan $\theta$ |
| weighting scheme[a] | | $w = 4(F_o)^2/[\sigma(F_o)^2]^2$ | |
| no. of std ref | 3 | 3 | 3 |
| variatn in std intens, % | ±0.6 | ±1.6 | ±0.1 |
| no. of unique data collected | 3654 | 3682 | 838 |
| no. of data used in refinement, $I > 3\sigma(I)$ | 3436 | 3366 | 818 |
| data:parameter ratio | 14.6 | 15.8 | 9.1 |
| final GOF | 1.62 | 2.10 | 1.85 |
| final $R_F$, $R_{wF}$ | 0.028 (0.044) | 0.029 (0.052) | 0.035 (0.047) |
| systematic absences obsd | none | none | $hkl$, $h+k+l = 2n+1$ |
| data collected | $\pm h,\pm k,l$ | $h,\pm k,\pm l$ | $hkl$ |
| final largest shift/esd | 0.01 | 0.01 | 0.04 |
| highest peak in final diff map, e/Å$^3$ | 0.63 | 0.75 | 0.76 |

[a] $[\sigma(F_o)^2]^2 = [S^2(C + R^2B) + (rF_0^2)^2]/(\mathrm{Lp})^2$, where $S$ is the scan rate, $C$ is the integrated peak count, $R$ is the ratio of scan to background counting time, $B$ is the total background count, and $r$ is a factor used to downweight intense reflections. For these structures, $r = 0.04$.

thiophene complex have been calculated with the semiempirical INDO/S method. Corresponding studies of the Ru(II) complexes are in progress and will be reported elsewhere.

## Experimental and Computational Section

**1. Preparation of the Complexes.** Complexes **1**, $Ru(NH_3)_5SC_4H_8 \cdot 1.5S_2O_6 \cdot 3H_2O$, **2**, $Ru(NH_3)_5S(CH_3)(C_2H_5) \cdot 1.5PF_6 \cdot 1.5F$, and **3**, $Ru(NH_3)_5S(CH_3)_2 \cdot 2Cl \cdot PF_6$, were prepared by a published method[8] using some modifications to obtain single crystals. In a typical preparation for **1** or **2**, 100 mg (0.34 mmol) of $[Ru(NH_3)_5Cl]Cl_2$ was added to 79 mg (0.34 mmol) of $Ag_2O$ dissolved in 0.5 mL of 2 M trifluoroacetic acid (HTFA) to precipitate ionic chloride. Following adjustment of the pH to 1 by the addition of water (5–8 mL) and the removal of AgCl by filtration, zinc amalgam was added under Ar for 15 min to reduce Ru(III) to Ru(II). A 5–10-fold excess of thioether was added and the solution was allowed to stand for ca. 30 min.

The Ru(II) dithionate precursor of **1** was precipitated by adding 0.07 g of $Na_2S_2O_6$ and 15 mL of ethanol, collected by filtration, and dissolved in 10 mL of $H_2O$, to which was added 0.032 g of $Na_2S_2O_6$ and several drops of 2 M HTFA to adjust the pH to 1. Air oxidation for 12–16 h at room temperature gave the Ru(III) salt. Slow vapor diffusion of ethanol into an aqueous solution of the complex yielded orange crystals of **1** suitable for X-ray diffraction studies.

The Ru(II) hexafluorophosphate precursor of **2** was prepared by a similar procedure, precipitated by adding excess (1.5 g) $NH_4PF_6$, collected, dissolved in a minimum amount of acetone (to remove occluded ligand), and reprecipitated by adding 5 mL of aqueous 60% $HPF_6$. The Ru(II) salt was dissolved in a minimum amount of water (ca. 10 mL). Several drops of $HPF_6$ were added and the solution was allowed to oxidize in air as above. Crystals of **2** suitable for X-ray diffraction studies were grown by slow vapor diffusion of ethanol into an aqueous solution of the complex. X-ray analysis (see below) revealed **2** to be a mixed hexafluorophosphate–fluoride salt; the origin of fluoride was the HF present in aqueous $HPF_6$.

The Ru(II) hexafluorophosphate precursor of **3**, prepared by a published method,[8] was dissolved in a minimum amount of dilute (ca. 0.05 M) HCl, air oxidized for 1 h to a golden-yellow color, and filtered. Slow evaporation of the filtrate in air yielded diffraction quality crystals. X-ray analysis (see below) showed **3** to be an intimately twinned, mixed chloride–hexafluorophosphate salt. The complex **3** was prepared before **1** or **2**. To remove chloride as a potential anion, HCl was avoided in succeeding preparations.

**2. Spectroscopic Measurements.** Electronic spectral measurements were made using a computer-interfaced spectrophotometer built by Aviv Associates that utilizes a Cary Model 14 monochromator and cell compartment. Low-temperature spectra (80 K) were measured in $CH_3OH/H_2O$ glasses using an Air Products optical Dewar. The glasses were formed between circular quartz windows separated by rubber spacers.

**3. X-ray Diffraction Studies.** All diffraction measurements were made on an Enraf-Nonius CAD-4 diffractometer with graphite monochromated Mo K$\alpha$ radiation. The Enraf-Nonius Structure Determination Package[15] was used for data collection, processing, and structure solution. Crystal data and additional details of the data collection and refinement for the three crystals studied are presented in Table I. For each crystal, intensity data were corrected for decay, absorption (empirical), and Lp effects. The structures were solved by direct methods[16] and refined on $F$ by using full-matrix least-squares techniques. H-atom temperature factors were set equal to $1.3B_N$, where N is the atom bonded to H.

A crystal of **1**, $Ru(NH_3)_5SC_4H_8 \cdot 1.5S_2O_6 \cdot 3H_2O$, was mounted inside a glass capillary that contained a small amount of mother liquor well removed from the crystal. An E map based on 394 phases revealed the Ru and several ligand atoms; the remaining non-hydrogen atoms were located on successive difference Fourier maps. Following refinement of the non-hydrogen atoms, several H atoms were located from a difference map. Coordinates for the remaining H atoms were calculated by as-

(15) Enraf-Nonius Structure Determination Package, Enraf-Nonius, Delft, Holland, 1983.

(16) Main, P.; Fiske, S. J.; Hull, S. E.; Lessinger, L.; Germain, G.; Declercq, J.-P.; Woolfson, M. M. MULTAN 82. A System of Computer Programs for the Automatic Solution of Crystal Structures from X-ray Diffraction Data. University of York, England and Louvain, Belgium, 1982.

**Table II.** Fractional Atomic Coordinates and Equivalent Isotropic Thermal Parameters for **1**[a]

| | x | y | z | B or $B_{eq}$ (Å$^2$) |
|---|---|---|---|---|
| Ru(1) | 0.16562 (2) | 0.25771 (2) | 0.08963 (3) | 1.891 (4) |
| S(1) | 0.25964 (8) | 0.11205 (6) | 0.1681 (1) | 2.64 (2) |
| N(1) | 0.1038 (3) | 0.2678 (2) | 0.3054 (3) | 2.89 (6) |
| N(2) | 0.3627 (3) | 0.3665 (2) | 0.2527 (4) | 3.11 (6) |
| N(3) | 0.0690 (3) | 0.3822 (2) | 0.0171 (4) | 2.73 (6) |
| N(4) | −0.0351 (3) | 0.1522 (2) | −0.0767 (4) | 2.89 (6) |
| N(5) | 0.2181 (3) | 0.2558 (2) | −0.1332 (3) | 2.92 (6) |
| C(1) | 0.3764 (4) | 0.1347 (3) | 0.4111 (5) | 4.45 (9) |
| C(2) | 0.5260 (5) | 0.1351 (5) | 0.4268 (7) | 6.3 (1) |
| C(3) | 0.5171 (4) | 0.0712 (4) | 0.2626 (6) | 5.7 (1) |
| C(4) | 0.4020 (4) | 0.0921 (3) | 0.1001 (5) | 4.29 (8) |
| S(2) | 0.08144 (8) | 0.97131 (6) | 0.5951 (1) | 2.53 (2) |
| S(3) | 0.67301 (9) | 0.27276 (7) | −0.0323 (1) | 3.11 (2) |
| S(4) | 0.74684 (8) | 0.41521 (7) | 0.1641 (1) | 2.93 (2) |
| O(1) | 0.7447 (3) | 0.2907 (2) | −0.1469 (3) | 4.07 (6) |
| O(2) | 0.5183 (3) | 0.2616 (2) | −0.1233 (4) | 4.62 (7) |
| O(3) | 0.7219 (3) | 0.1968 (2) | 0.0679 (4) | 5.39 (8) |
| O(4) | 0.9018 (3) | 0.4255 (2) | 0.2611 (4) | 4.08 (7) |
| O(5) | 0.7068 (3) | 0.4930 (2) | 0.0600 (4) | 4.40 (7) |
| O(6) | 0.6701 (3) | 0.4024 (3) | 0.2741 (3) | 5.18 (7) |
| O(7) | 0.0281 (3) | 0.9532 (2) | 0.7304 (3) | 3.95 (6) |
| O(8) | 0.2103 (3) | 1.0530 (2) | 0.6641 (4) | 4.06 (7) |
| O(9) | 0.0869 (3) | 0.8776 (2) | 0.4875 (4) | 4.21 (7) |
| O(10) | 0.6236 (3) | 0.6179 (2) | 0.3647 (4) | 4.65 (7) |
| O(11) | 0.0309 (4) | 0.6649 (2) | 0.3922 (4) | 5.72 (9) |
| O(12) | 0.2757 (4) | 0.5548 (3) | 0.3495 (4) | 6.00 (9) |

[a] Anisotropically refined atoms are given in the form of the isotropic equivalent displacement parameter defined as $(^4/_3)[a^2B(1,1) + b^2B(2,2) + c^2B(3,3) + ab(\cos\gamma)B(1,2) + ac(\cos\beta)B(1,3) + bc(\cos\alpha)B(2,3)]$.

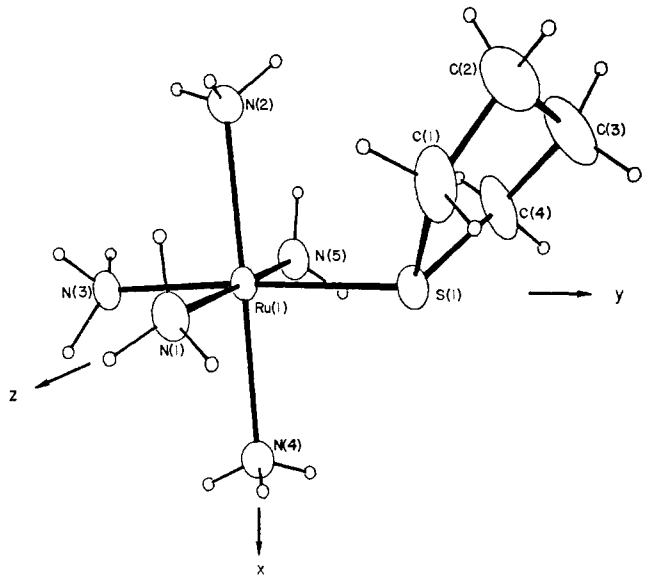


**Figure 1.** View of the cation in **1** showing the atom numbering scheme and the coordinate axes for the molecular orbital calculations.

suming idealized bond geometries except for three water H atoms which were not included in the structure. H-atom parameters were not refined. Anisotropic refinement proceeded smoothly and led to convergence with $R_F$ and $R_{wF}$ equal to 0.028 and 0.044, respectively.

A crystal of **2**, $Ru(NH_3)_5S(CH_3)(C_2H_5)\cdot1.5PF_6\cdot1.5F$, was mounted on the end of a glass rod. An E map based on 301 phases revealed the Ru and several ligand atoms. The remaining non-hydrogen atoms were located on successive difference maps. H atoms were added to the structure as in **1** and were not refined. One $PF_6$ anion was located on a general position and showed no disorder, while the second was situated on a center of symmetry and exhibited a two-site positional disorder in the equatorial plane. The lattice F atoms also showed positional disorder, which was modeled by four F atoms on partially occupied sites. Refinement led to convergence with $R_F$ and $R_{wF}$ equal to 0.029 and 0.052, respectively.

A crystal of **3**, $Ru(NH_3)_5S(CH_3)_2\cdot2Cl\cdot PF_6$, was mounted on the end of a glass fiber. Diffractometer examination of the reciprocal lattice revealed *mmm* Laue symmetry and systematic absences consistent with the body-centered orthorhombic space groups *I*222 (No. 23), $I2_12_12_1$ (No. 24), *Imm*2 (No. 44), and *Immm* (No. 71). The structure was solved and refined in the noncentrosymmetric space group *Imm*2. Examination of the structure (see below) revealed that the crystals are intimately twinned with individual end-centered monoclinic cells related by a mirror plane twinning element to give apparent orthorhombic symmetry.

An E map based on 131 phases revealed the unique Ru, Cl, and P atoms. The remaining non-hydrogen atoms were located readily from successive difference maps, except for the S atom which appeared at half-height on a 4c site (*m* symmetry) in *Imm*2. The mirror plane relating the two half-height S atoms is the twin plane. This plane was found to contain 7 of the 10 unique non-hydrogen atoms in the structure, including the Ru atom and the methyl C atom C(1). Anisotropic refinement proceeded smoothly and led to convergence with $R_F = 0.035$ and $R_{wF} = 0.047$. The C–S bond length in **3** appeared to be unusually short and the temperature factor of the C atom appeared to be anomalously high compared with the value for the S atom to which it is bonded. Examination of the electron density around the C atom revealed substantially greater extension perpendicular to the twin plane than parallel to it, suggesting that the C atom lies near, rather than on, the twin plane. Two half-height C atoms with *x* coordinates of ±0.030 are also consistent with the electron density, and these atoms give C–S bond distances (1.814 Å) consistent with those observed in similar structures such as **1** and **2**.

**Table III.** Fractional Atomic Coordinates and Equivalent Isotropic Thermal Parameters for **2**[a]

| | x | y | z | B or $B_{eq}$ (Å$^2$) | mult |
|---|---|---|---|---|---|
| Ru(1) | 0.32484 (2) | −0.19419 (2) | −0.35151 (2) | 1.407 (4) | |
| S(1) | 0.27195 (7) | −0.39082 (6) | −0.49574 (8) | 1.97 (1) | |
| N(1) | 0.4181 (2) | −0.2091 (2) | −0.5734 (3) | 2.05 (5) | |
| N(2) | 0.1366 (2) | −0.0859 (2) | −0.4239 (3) | 2.35 (5) | |
| N(3) | 0.3800 (2) | −0.0199 (2) | −0.2370 (3) | 2.21 (5) | |
| N(4) | 0.5157 (2) | −0.2940 (2) | −0.2694 (3) | 2.45 (5) | |
| N(5) | 0.2373 (3) | −0.1741 (2) | −0.1229 (3) | 2.45 (5) | |
| C(1) | 0.1584 (4) | −0.3718 (3) | −0.6810 (4) | 3.04 (7) | |
| C(2) | 0.1307 (4) | −0.4961 (4) | −0.7940 (5) | 4.05 (8) | |
| C(4) | 0.1622 (3) | −0.4264 (3) | −0.3741 (4) | 3.30 (7) | |
| P(1) | 0.77966 (7) | 0.88942 (7) | 0.68716 (9) | 2.18 (1) | |
| P(2) | 0.500 | 0.500 | 0.500 | 2.20 (2) | 0.50 |
| F(1) | 0.8747 (2) | 0.8510 (2) | 0.5179 (2) | 3.41 (4) | |
| F(2) | 0.7620 (2) | 0.7417 (2) | 0.6271 (3) | 4.39 (5) | |
| F(3) | 0.9221 (2) | 0.8527 (2) | 0.8074 (3) | 4.05 (5) | |
| F(4) | 0.6832 (2) | 0.9286 (2) | 0.8582 (2) | 3.49 (4) | |
| F(5) | 0.7927 (2) | 1.0392 (2) | 0.7420 (2) | 3.45 (4) | |
| F(6) | 0.6360 (2) | 0.9301 (2) | 0.5675 (2) | 3.25 (4) | |
| F(7) | 0.4988 (2) | 0.5273 (2) | 0.2142 (2) | 3.23 (4) | |
| F(8) | 0.5599 (3) | 0.6278 (2) | 0.0350 (3) | 5.03 (7) | 0.70 |
| F(9) | 0.3419 (3) | 0.5926 (3) | −0.0008 (4) | 5.28 (8) | 0.70 |
| F(10) | 0.9220 (3) | 0.8449 (2) | 0.1449 (3) | 4.55 (7) | 0.80 |
| F(11) | 0.7790 (6) | −0.2950 (5) | −0.7909 (6) | 5.6 (1) | 0.40 |
| F(8P) | 0.4210 (8) | 0.6536 (7) | 0.029 (1) | 4.3 (1)* | 0.30 |
| F(9P) | 0.3526 (8) | 0.4737 (7) | −0.016 (1) | 4.9 (2)* | 0.30 |
| F(11P) | 0.800 (1) | 0.675 (1) | 0.240 (2) | 4.0** | 0.15 |
| F(11PP) | 0.733 (1) | 0.734 (1) | 0.216 (2) | 4.0** | 0.15 |

[a] Starred atoms were refined isotropically; temperature factors for doubly starred atoms were not refined. Anisotropically refined atoms are given in the form of the isotropic equivalent displacement parameter defined as $(4/3)[a^2B(1,1) + b^2B(2,2) + c^2B(3,3) + ab(\cos\gamma)B(1,2) + ac(\cos\beta)B(1,3) + bc(\cos\alpha)B(2,3)]$.

**Table IV.** Fractional Atomic Coordinates and Equivalent Isotropic Thermal Parameters for **3**[a]

| | x | y | z | B or $B_{eq}$ (Å$^2$) | mult[b] |
|---|---|---|---|---|---|
| Ru | 0.000 | 0.000 | 0.766 | 2.051 (7) | 0.25 |
| S(1) | −0.0717 (4) | 0.000 | 1.0249 (3) | 2.51 (4) | 0.25 |
| N(1) | −0.1925 (5) | 0.1355 (3) | 0.7563 (5) | 3.24 (6) | 1.00 |
| N(3) | 0.000 | 0.000 | 0.5305 (8) | 2.09 (9) | 0.25 |
| C(1) | 0.000 | −0.1270 (8) | 1.120 (1) | 6.2 (3) | 0.50 |
| Cl | 0.000 | 0.3035 (2) | 0.4969 (2) | 2.94 (2) | 0.50 |
| P | 0.500 | 0.000 | 0.4258 (3) | 2.70 (4) | 0.25 |
| F(1) | 0.500 | 0.000 | 0.6114 (9) | 4.6 (1) | 0.25 |
| F(2) | 0.3507 (5) | 0.1076 (4) | 0.4247 (6) | 4.95 (8) | 1.00 |
| F(3) | 0.000 | 0.500 | 0.7228 (9) | 7.4 (3) | 0.25 |

[a] Anisotropically refined atoms are given in the form of the isotropic equivalent displacement parameter defined as $(4/3)[a^2B(1,1) + b^2B(2,2) + c^2B(3,3) + ab(\cos\gamma)B(1,2) + ac(\cos\beta)B(1,3) + bc(\cos\alpha)B(2,3)]$. [b] Atom multiplier.

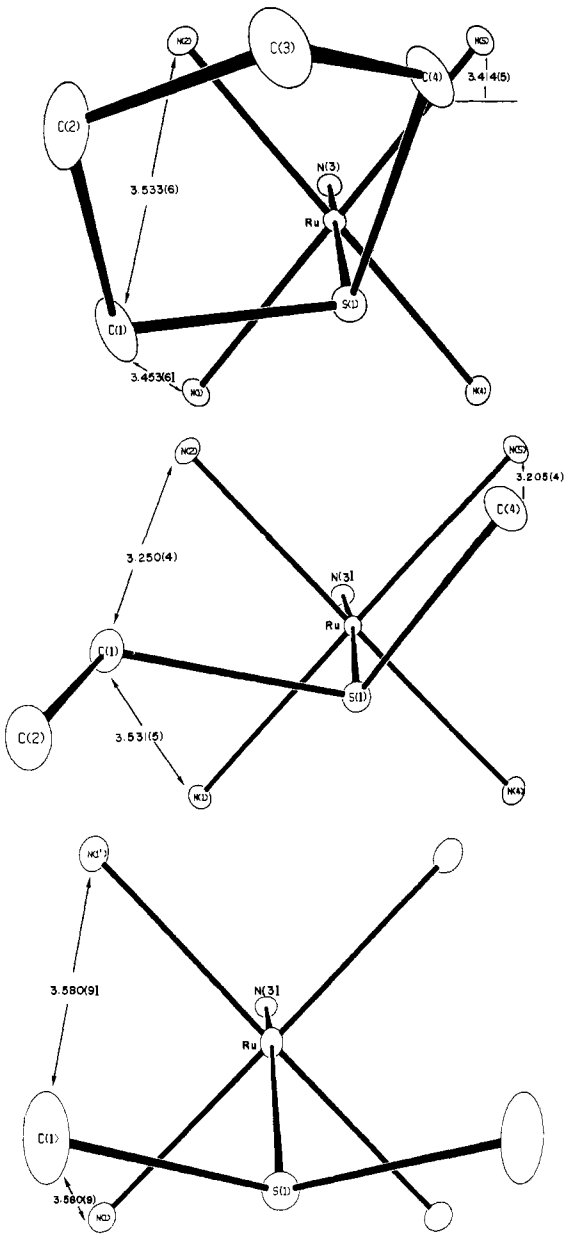


**Figure 2.** Views of the cations in (a, top) complex **1**, (b, middle) complex **2**, and (c, bottom) complex **3** showing the relative orientation of the thioether and $A_5Ru$ moieties. Short nonbonding C···N distances are also indicated. For complex **3**, only one component of the twin is shown and the C atom is that which was crystallographically refined.

Final atomic parameters for **1–3** are given in Tables II–IV, respectively. A view of the cation in **1**, showing the atom numbering scheme and the coordinate axes used for the molecular orbital calculations, is given in Figure 1. Views of the cations in **1–3**, showing the orientation of the thioether and $(NH_3)_5Ru$ groups, are shown in Figure 2, while a view of the cation in **3**, showing the twin plane and the apparent S–C bond length, is given in Figure 3a. Figure 3b shows the relationship of the end-centered monoclinic cells and the twinned body-centered orthorhombic cell. Lists of anisotropic thermal parameters, H atom coordinates, and observed and calculated structure factors are available.[17]

**4. Computational Details.** We have carried out ab initio molecular orbital calculations on the electronic ground states of $(NH_3)_5Ru(III)S(CH_3)_2$, $NH_3$, and $S(CH_3)_2$ using an extended version of the GAMESS electronic structure program package.[18] Wave functions for closed shell singlet states [$NH_3$, $S(CH_3)_2$] were generated with the standard single determinant restricted Hartree–Fock method of Roothaan,[19a] whereas the

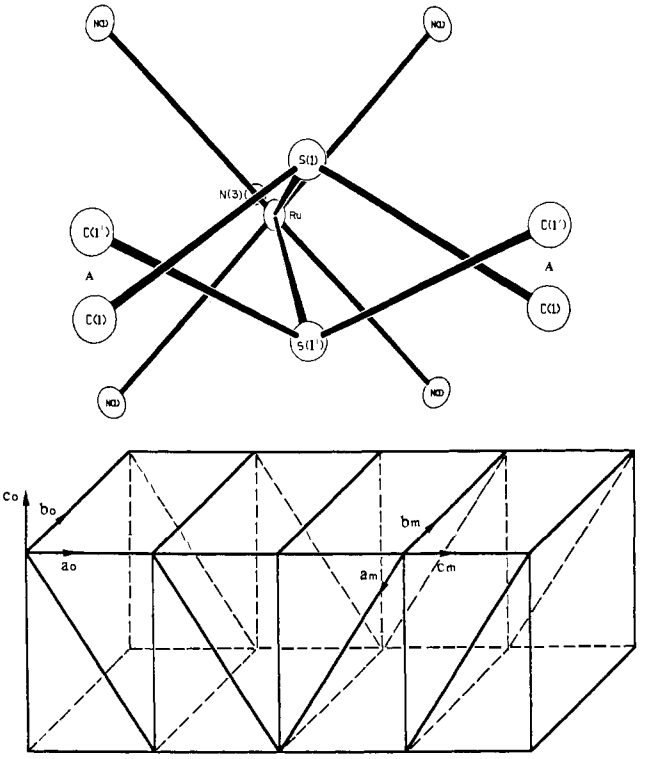


**Figure 3.** (a, top) View of the twinned cation in **3**. The carbon atom C(1) is shown with an $x$ coordinate of 0.030, 0.33 Å removed from the $b_oc_o$ twin plane. The twin plane causes the apparent position of C(1) to appear as A with consequent distortion of the dimethyl thioether geometry. (b, bottom) Sketch of four unit cells of **3** showing the relation between the individual end-centered monoclinic cells and the twinned body-centered orthorhombic cell. The subscripts o and m refer to the orthorhombic and monoclinic cells, respectively.

unrestricted procedure due to Pople and Nesbet[19b] was used for doublet states $[(NH_3)_5Ru^{III}S(CH_3)_2]$. Electronic population indices were derived by the procedures proposed by Weinhold et al.[19c]

The inner core electrons for Ru ($1s^22s^22p^63s^23p^63d^{10}4s^24p^6$), S ($1s^22s^22p^6$), N ($1s^2$), and C ($1s^2$) were replaced by ab initio effective core potentials (ECPs). For Ru, S, and C we used the relativistic ECPs developed by Christiansen and Ermler,[20a,b] whereas for N we used the nonrelativistic ECP developed by Stevens, Basch, and Krauss.[20c] The valence electrons were described with the basis sets developed specifically for use with these potentials suitably augmented with polarization functions; for H, the minimal STO-3G basis set of Hehre, Stewart, and Pople was used.[20d] The Ru (5s, 5p, 4d) basis set[20a] was extended with an additional diffuse $d$ function (exponent = 0.08) and subsequently contracted as follows: (5s, 5p, 5d) → [3, 1, 1/4, 1/3, 1, 1]. Similarly, one set of diffuse $p$ functions (exponent = 0.05) and two sets of $d$ functions (exponents = 0.65[20e] and 0.15, respectively) were added to the S (4s, 4p) basis set[20b] and then contracted as follows: (4s, 5p, 2d) → [3, 1/3, 1, 1/1, 1]. The valence basis set for C[20b] was split to give a double-$\zeta$ type description (4s, 4p) → [3, 1/3, 1] but the N basis set[20c] was used uncontracted (4s, 4p) → [4/4]. These choices of basis sets lead to 45 and 107 basis functions for the dimethyl thioether molecule and $(NH_3)_5Ru$–dimethyl thioether complex, respectively. Geometry optimizations of the ligands [$C_{2v}$ symmetry for $S(CH_3)_2$, $C_{3v}$ for $NH_3$] and the Ru–thioether complex ($C_s$ symmetry) were carried out with these basis sets using Schlegel's scheme[19d] with analytical gradients and numerical, finite difference second derivatives. Amplitude contour plots of

(17) Supplementary material.

(18) Dupuis, M.; Spangler, D.; Wendoloski, J. GAMESS, NRCC Software Catalogue, Vol. 1, Program No. QG01, 1980. Schmidt, M. W.; Boatz, J. A.; Baldridge, K. K.; Koseki, S.; Gordon, M. S.; Elbert, S. T.; Lam, B., private communication. Stevens, W. J.; Krauss, M., private communication.

(19) (a) Roothaan, C. C. J. *Rev. Mod. Phys.* **1951**, *23*, 69. (b) Pople, J. A.; Nesbet, R. K. *J. Chem. Phys.* **1954**, *22*, 571. (c) Reed, A. E.; Weinhold, F. *J. Chem. Phys.* **1983**, *78*, 4066. Reed, A. E.; Weinstock, R. B.; Weinhold, F. *J. Chem. Phys.* **1985**, *83*, 735. (d) Schlegel, H. B. *J. Comput. Chem.* **1982**, *3*, 214. (e) Roothaan, C. C. J. *Rev. Mod. Phys.* **1960**, *32*, 179.

(20) (a) LaJohn, L. A.; Christiansen, P. A.; Ross, R. B.; Atashroo, T.; Ermler, W. J. *J. Chem. Phys.* **1987**, *87*, 2812. (b) Pacios, L. F.; Christiansen, P. A. *J. Chem. Phys.* **1985**, *82*, 2664. (c) Stevens, W. J.; Basch, H.; Krauss, M. *J. Chem. Phys.* **1984**, *81*, 6026. (d) Hehre, W. J.; Stewart, R. F.; Pople, J. A. *J. Chem. Phys.* **1969**, *51*, 2657. (e) Francl, M. M.; Pietro, W. J.; Hehre, W. J.; Binkley, J. S.; Gordon, M. S.; DeFrees, D. J.; Pople, J. A. *J. Chem. Phys.* **1982**, *77*, 3654.

Table V. Bond Distances (Å) and Angles (deg) in 1-3

| | 1 | 2 | 3[a] |
|---|---|---|---|
| Ru-S(1) | 2.3666 (7) | 2.3711 (5) | 2.384 (2) |
| Ru-N(1) | 2.111 (2) | 2.108 (2) | 2.111 (3) |
| Ru-N(2) | 2.107 (2) | 2.097 (2) | |
| Ru-N(3) | 2.109 (2) | 2.126 (2) | 2.100 (6) |
| Ru-N(4) | 2.115 (2) | 2.105 (2) | |
| Ru-N(5) | 2.110 (2) | 2.109 (2) | |
| S(1)-C(1) | 1.827 (3) | 1.822 (2) | 1.725 (6)[b] |
| S(1)-C(4) | 1.816 (3) | 1.805 (2) | |
| C(1)-C(2) | 1.501 (6) | 1.514 (4) | |
| C(2)-C(3) | 1.455 (6) | | |
| C(3)-C(4) | 1.491 (5) | | |
| S(1)-Ru-N(1) | 89.99 (7) | 89.36 (5) | 82.6 (1) |
| S(1)-Ru-N(2) | 94.65 (7) | 93.87 (5) | 101.8 (1) |
| S(1)-Ru-N(3) | 176.41 (6) | 176.08 (5) | 166.47 (6) |
| S(1)-Ru-N(4) | 87.06 (7) | 89.11 (5) | (82.6 (1)) |
| S(1)-Ru-N(5) | 94.21 (6) | 92.96 (5) | (101.8 (1)) |
| N(1)-Ru-N(2) | 91.6 (1) | 92.48 (7) | 90.3 (2) |
| N(1)-Ru-N(3) | 88.22 (9) | 86.74 (7) | 87.8 (1) |
| N(1)-Ru-N(4) | 88.42 (9) | 88.21 (7) | 89.5 (2) |
| N(1)-Ru-N(5) | 175.72 (9) | 177.42 (6) | 175.5 (3) |
| N(2)-Ru-N(3) | 88.52 (9) | 86.72 (7) | (87.8 (1)) |
| N(2)-Ru-N(4) | 178.30 (1) | 176.95 (7) | (175.5 (3)) |
| N(2)-Ru-N(5) | 88.9 (1) | 88.50 (7) | (89.5 (2)) |
| N(3)-Ru-N(4) | 89.78 (9) | 90.36 (7) | (87.8 (1)) |
| N(3)-Ru-N(5) | 87.54 (9) | 90.93 (7) | (87.8 (1)) |
| N(4)-Ru-N(5) | 91.0 (1) | 90.70 (8) | (90.3 (2)) |
| Ru-S(1)-C(1) | 112.1 (1) | 107.86 (8) | 113.8 (3)[b] |
| Ru-S(1)-C(4) | 114.5 (1) | 112.17 (8) | (113.8 (3))[b] |
| C(1)-S(1)-C(4) | 94.2 (2) | 100.7 (1) | 107.7 (5)[b] |
| S(1)-C(4)-C(3) | 105.1 (2) | 112.25 (8) | |
| C(4)-C(3)-C(2) | 109.5 (3) | | |
| C(3)-C(2)-C(1) | 109.8 (3) | | |
| C(2)-C(1)-S(1) | 105.9 (2) | | |

[a] For 3, the equatorial N atoms are equivalent by symmetry in the twinned structure. For this structure, N(2) = N(1′), N(4) = N(1″), N(5) = N(1‴), and C(4) = C(1′). Singly, doubly, and triply primed atoms are related, respectively, to unprimed atoms by the following symmetry transformations: $-x, y, z$; $x, -y, z$; and $-x, -y, z$. C(4) is related to C(1′) by $x, -y, z$. [b] These values were calculated by using the refined C(1) coordinates in Table IV. Owing to twinning, the true values may be substantially different (see the experimental section).

selected molecular orbitals were made from converged vectors at these optimized geometries.

Semiempirical molecular orbital calculations based on a modified INDO approach[21] were carried out on the electronically excited states of the tetrahydrothiophene ligand and its Ru complex (1) at the experimental geometries with a program described previously.[2,21] All Ru, N, C, and H parameters were identical with those applied earlier;[2] the parameters for S were as described in ref 21b except that the ionization potential for the S 3p orbitals [EI(p)] was increased from −12.39 to −9.39 eV.[22-24] The ground-state wave functions were generated by restricted closed[19a] or open[21c,f] shell methods. The excited states were then obtained from configuration interaction (CI) calculations using configurations singly excited relative to the ground state. Only configurations preserving the spin orientation of the promoted electron were considered in the CI calculations on the excited doublet states of the complex. Nearly 200 configurations were included and it was ascertained that satisfactory convergence in the calculated properties had been obtained with this level of CI. Calculated oscillator strengths include the one-center atomic sp and pd terms in the dipole-length approximation.

## Results and Discussion

**Crystal Structures.** The structures of 1-3 each contain $A_5Ru^{III}L^{3+}$ cations [A = $NH_3$, L = tetrahydrothiophene (1), methyl ethyl thioether (2), or dimethyl thioether (3)] separated by various anions and, in the case of 1, lattice water molecules. In each structure, five $N(NH_3)$ atoms and the S atom from the ligand L complete a distorted octahedron about Ru. Bond distances and angles (Table V) show that the coordination geometries of 1 and 2 are strikingly similar: corresponding bond distances are equivalent to ±0.01 Å, while corresponding bond angles in the coordination sphere differ on average by 1.1° with the largest difference equal to 3.4°. The cation in the twinned structure 3 shows Ru-N and Ru-S bond distances comparable to those in 1 and 2, but much larger angular deviations from ideal octahedral values within the coordination sphere, particularly for those angles involving the S atom. In 3, the S atom is moved away from two "equatorial" N(amine) atoms toward the remaining two in such a way as to reduce the trans N(3)-Ru-S(1) angle from approximately 176° in 1 to 166°. This distortion occurs without significant changes in the Ru-S or Ru-N bond distances and may be related to the relative orientation of the thioether ligands and the $A_5Ru^{III}$ units (see Figure 2). For 1 and 2, one of the C atoms bonded to S approximately eclipses an equatorial N(amine) atom, while the other is approximately staggered with respect to the equatorial N atoms. This configuration gives rise to three short nonbonded intramolecular C···N contacts (Figure 2). In contrast, for 3, a crystallographic mirror plane bisects the C-S-C angle and the dimethyl thioether C atoms are more symmetrically disposed with respect to the equatorial N(amine) atoms. The relative orientation of the $SC_2$ and $A_5Ru^{III}$ units (Figure 2c) is such that the C···N distances are equal. To maintain this geometry while maximizing bonding with Ru, the S atoms must be located at a position that leads to a relatively small trans N(3)-Ru-S(1) angle.

The Ru-N distances compare favorably with those in other structures containing $A_5Ru^{III}$ units such as $[A_5Ru^{III}(pyrazine)RuA_5]^{n+}$, $n$ = 5, 6[25] [range 2.090 (1)-2.135 (3) Å] and $A_5Ru^{III}(hyp)^{3+}$ and $A_5Ru^{III}(7\text{-Mehyp})^{3+}$ [range 2.081 (9)-2.115 (7) Å, hyp = hypoxanthine].[26] The Ru-S(thioether) distances in 1-3 span a small range [2.3666 (7)-2.384 (2) Å, Table V] and are equivalent to within ±0.01 Å. To our knowledge, these complexes provide the first structural characterization of the Ru(III)-S(thioether) linkage. Several complexes containing Ru(III)-S(dithiocarbamate) bonds have been characterized structurally;[27] terminal Ru(III)-S bonds range from 2.368 (4) to 2.433 (11) Å and are similar in length to those in the present structures. In contrast, the Ru(II)-S(thioether) distance in $A_5Ru^{II}S(CH_3)_2 \cdot 2PF_6$, the Ru(II) analogue of 3,[28a] is considerably shorter [2.316 (3) Å], presumably owing to back-bonding involving donor Ru d($\pi$) orbitals and thioether acceptor orbitals. In the recently reported[28b] structure of $Ru^{II}(OEP)(SPh_2)_2$, where OEP is the dianion of octaethylporphyrin, the diphenyl thioether ligands

(21) The original procedures and parameters are described in: (a) Zerner, M. C.; Loew, G. H.; Kirchner, R. F.; Mueller-Westerhoff, U. T. *J. Am. Chem. Soc.* **1980**, *102*, 589. (b) Herman, Z. S.; Kirchner, R. F.; Loew, G. H.; Mueller-Westerhoff, U. T.; Nazzal, A.; Zerner, M. C. *Inorg. Chem.* **1982**, *21*, 46. (c) Anderson, W. P.; Edwards, W. D.; Zerner, M. C. *Inorg. Chem.* **1986**, *25*, 2728. (d) Bacon, A. D.; Zerner, M. C. *Theor. Chim. Acta* **1979**, *53*, 21. (e) Ridley, J.; Zerner, M. *Theor. Chim. Acta* **1973**, *32*, 111. (f) Edwards, W. D.; Zerner, M. C. *Theor. Chim. Acta* **1987**, *72*, 347.

(22) Frost, D. C.; Herring, F. G.; Katrib, A.; McDowell, C. A.; McLean, R. A. N. *J. Phys. Chem.* **1972**, *76*, 1036. Cradock, S.; Whiteford, R. A. *J. Chem. Soc., Faraday Trans. 2* **1972**, *68*, 281.

(23) With the parameters proposed in ref 21b we calculate the three highest lying MOs in thioether at −10.34, −12.28, and −13.36 eV. The 3.0-eV increase in EI(p) for S changes these values to −8.68, −11.25, and −12.55 eV, respectively, which using Koopmans' theorem,[24] compare very favorably with the measured ionization potentials of 8.65, 11.2, and 12.6 eV. We have found that it is of utmost importance to place the occupied ligand orbitals at proper energies in order to predict ligand to metal charge-transfer energies reliably; see also ref 2.

(24) Koopmans, T. *Physica (Utrecht)* **1934**, *1*, 104.

(25) Furholz, U.; Burgi, H.-B.; Wagner, F. E.; Stebler, A.; Ammeter, J. H.; Krausz, E.; Clark, R. J. H.; Stead, M. J.; Ludi, A. *J. Am. Chem. Soc.* **1984**, *106*, 121.

(26) Kastner, M. E.; Coffey, K. F.; Clarke, M. J.; Edmonds, S. E.; Eriks, K. *J. Am. Chem. Soc.* **1981**, *103*, 5747.

(27) (a) Pignolet, L. H. *Inorg. Chem.* **1974**, *13*, 2051. (b) Raston, C. L.; White, A. H. *J. Chem. Soc., Dalton Trans.* **1975**, 2405. (c) Raston, C. L.; White, A. H. *J. Chem. Soc., Dalton Trans.* **1975**, 2410. (d) Mattson, B. M.; Heiman, J. R.; Pignolet, L. H. *Inorg. Chem.* **1976**, *15*, 564.

(28) (a) The X-ray crystal structure of a twinned crystal of $A_5Ru^{II}S(CH_3)_2 \cdot 2PF_6$ has been determined and refined to current values of $R_F$ and $R_{wF}$ of 0.058 and 0.083, respectively. Crystallography: $RuSP_2F_{12}N_5C_2H_{21}$, monoclinic, $P2_1/n$, $a$ = 8.5950 (7) Å, $b$ = 12.265 (1) Å, $c$ = 16.958 (2) Å, $\beta$ = 101.478 (8)°, $Z$ = 2, $d_{obsd}$ = 2.03 (1) g/cm$^{-3}$, $d_{calcd}$ = 2.04 g/cm$^{-3}$. The structure was solved by using 2359 reflections with $I > 3\sigma(I)$ (Mo K$\alpha$ radiation) and refined by full-matrix least-squares techniques. Complete details of the structure determination will be published elsewhere. (b) James, B. R.; Pacheco, A.; Rettig, S. J.; Ibers, J. A. *Inorg. Chem.* **1988**, *27*, 2414.

**Table VI.** Calculated and Experimental Geometries of Dimethyl Thioether and $[(NH_3)_5RuSR_2]^{3+}$ Complexes[a]

| | $S(CH_3)_2$ | | complex | |
|---|---|---|---|---|
| | calcd[b] | ED[c] | calcd[b] | X-ray |
| S-C | 1.805 | 1.805 | 1.842 | 1.825 (4)[d] |
| C-S-C | 100.7 | 99.1 | 104.8 | 100.7 (1)[e] |
| Ru-S | | | 2.435 | 2.374 (9)[d] |
| Ru-N(1) | | | 2.128 | 2.110 (3)[f] |
| Ru-N(2) | | | 2.108 | 2.105 (3)[f] |
| Ru-N(3) | | | 2.131 | 2.112 (5)[f] |
| Ru-N(4) | | | 2.087 | 2.110 (3)[f] |
| Ru-N(5) | | | 2.128 | 2.110 (3)[f] |
| S-Ru-N(2) | | | 99.2 | 92.0 (6)[d] |
| S-Ru-N(3) | | | 172.4 | 176.3 (2)[d] |
| S-Ru-N(4) | | | 84.1 | 88.1 (15)[d] |
| Ru-S-X[g] | | | 139.4 | 123.8[d] |

[a] Bond lengths in angstroms, angles in degrees. [b] Ab initio structure of $(NH_3)_5RuS(CH_3)_2$, this work. [c] Electron diffraction structure, ref 29. [d] Average values for **1** and **2**, this work. Values for **3** were not included because of possible errors in parameters involving the C or S atoms arising from twinning. See text. [e] Value for **2**, this work. [f] Average of values for **1**-**3**. [g] X is a point on the CSC bisector; see text.

are trans and the Ru(II)-S(thioether) distances [2.376 (1), 2.361 (1) Å] are close to those observed for **1**-**3**. Longer Ru-S(thioether) bonds in the OEP complex are consistent with reduced back-bonding expected when a thioether ligand is trans to a second $\pi$-accepting ligand.

Bond distances within the ligands in **1** and **2** are typical. In particular, the S-C bond lengths [1.805 (2)-1.827 (3) Å] are quite close to the value of 1.807 (2) Å reported[29] for the free ligand $S(CH_3)_2$ and lie within the range 1.762 (11)-1.93 (2) Å reported[30] for several metal complexes containing bound tetrahydrothiophene (THT) or thioether ligands. The C-S-C angle in **1** [94.2 (2)°] is close to those reported for other THT-containing complexes [92.3 (3),[30a] 93.3 (3), 93.8 (3),[30b] 92.4 (6)° [30c]], while the corresponding angle in **2** [100.7 (1)°] is typical of those found in free[29] [99.05 (4)°] or bound[30d] [99.3 (9), 99.4 (4), 100.8 (5)°] thioethers. The smaller value of the C-S-C angle in **1** results from constraints imposed by the five-membered THT ring. The THT ring in **1** exists in the envelope conformation: atoms S(1), C(1), C(2), and C(4) are planar to ±0.04 Å, while C(3) deviates from this plane by 0.519 (6) Å. Atoms C(2) and C(3) in the THT ring exhibit relatively high thermal parameters (Table II) with thermal ellipsoids (Figure 1) whose principal axes are approximately perpendicular to the ring plane. As has been observed previously with a $Ru^{II}$(THT) complex,[30a] this thermal motion is consistent with a vibrational mode that would convert the envelope to the half-chair conformation.

The thioether ligands in **1** and **2** bond to Ru(III) with pyramidal coordination about S(1). Both show the S atom below the plane defined by Ru(1), N(1), N(3), and N(5) while the C atoms bonded to S, C(1), and C(4) are above this plane. In both structures, the C(1)-S(1)-C(4) plane is tilted with respect to the plane of the ammines cis to S. An estimate of this tilt is given by the Ru(1)-S(1)-X angle, where X is the midpoint of the C(1)···C(4) vector (Figure 1). These angles, 125.5 and 122.1° for **1** and **2**, respectively, are somewhat smaller than the values of 132.0 and 130.1° reported[31] for a Ru(II) complex containing a planar S-bound dibenzothiophene ligand. We attribute this tilt as well as the nonlinearity of the N(trans)-Ru-S group to a tradeoff between the bonding requirements of the thioether ligand and steric repulsions between the cis ammines and the thioether. As discussed below, the highest occupied molecular orbital in a thioether is essentially a S 3p orbital that is perpendicular to the $SC_2$ plane. In forming the Ru-S bond, this S 3p HOMO would be expected to interact with a vacant Ru d($\sigma$) orbital to form the $\sigma$ bond. The $\sigma$ bond of maximum strength would be expected to form with a Ru-S-X angle of 90° and with the $SC_2$ and cis ammine planes parallel, as in **4**. However, steric interactions

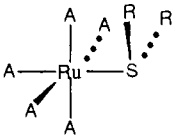


**4**

between the cis ammines and the methyl or methylene groups of the thioether ligand force the $SC_2$ plane to tilt away from this ideal geometry and, to maintain the overlap between the S 3p and Ru d($\sigma$) orbitals and/or reduce the strain, the N(trans)-Ru-S angle is reduced slightly from 180° (**5**). When steric constraints

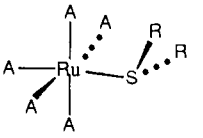


**5**

are less demanding, as in the Cu(II) complex[32] bis($\beta$-methylmercaptoamine)copper(II) diperchlorate that contains equatorially bound thioether and weak axial ligation by $ClO_4^-$ (**6**), the Cu-S-X angle is reduced to 107.9°.

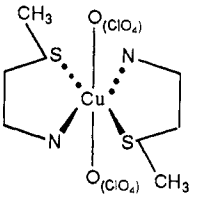


**6**

**Ground-State Electronic Structure.** The optimized geometries of free dimethyl thioether and the $[A_5Ru^{III}S(CH_3)_2]^{3+}$ complex from ab initio molecular orbital (MO) calculations incorporating effective core potentials and extended valence basis sets (see computational details section) are listed in Table VI along with pertinent experimental data. The coordinate system is chosen (Figure 1) so that the symmetry plane ($xy$) of the complex bisects the C-S-C angle and contains the N(2), N(3), N(4), Ru, and S atoms with the coordinate axes essentially directed along N(2)-Ru-N(4) ($x$), N(3)-Ru-S ($y$), and N(5)-Ru-N(1) ($z$) (Figure 1). The ground state of the complex ($^2A'$) has the unpaired electron residing in an orbital that is almost exclusively $4d_{xy}$ in character. The expectation value of $S^2$ (0.759) is only slightly larger than the value associated with a pure doublet (0.750), and thus very little spin contamination occurs from mixing with higher lying spin states. At the optimized $^2A'$ geometry, the two $^2A''$ states, which arise from the alternative occupancies of the d orbitals ($d_{xz}$, $d_{yz}$) within the $t_{2g}$ set, are calculated to be 1100-2000 $cm^{-1}$ (3-6 kcal/mol) higher in energy. The optimized geometry shows significant distortions from perfect octahedral coordination only in the direction of the Ru-S ligation site. The Ru-N bond length in $Ru(NH_3)_6^{3+}$ deduced from X-ray diffraction is 2.104 (4) Å[33] and the calculated Ru-N bond lengths in our complex all lie in the range 2.09-2.13 Å; also, all the N-Ru-N bond angles are within a few degrees of the ideal value for an octahedron. However, the computed Ru-S distance is much longer

(29) Iijima, T.; Tsuchiya, S.; Kimura, M. *Bull. Chem. Soc. Jpn.* **1977**, *50*, 2564.

(30) (a) Riley, D. P.; Oliver, J. D. *Inorg. Chem.* **1986**, *25*, 1825. (b) Ainscough, E. W.; Brodie, A. M.; Husbands, J. M.; Gainsford, G. J.; Gabe, E. J.; Curtis, N. F. *J. Chem. Soc., Dalton Trans.* **1985**, 151. (c) Mashiko, T.; Reed, C. A.; Haller, K. J.; Kastner, M. E.; Scheidt, W. R. *J. Am. Chem. Soc.* **1981**, *103*, 5758. (d) Coll, R. K.; Fergusson, J. E.; McKee, V.; Page, C. T.; Robinson, W. T.; Keong, T. S. *Inorg. Chem.* **1987**, *26*, 106.

(31) Bucknor, S. M.; Draganjac, M.; Rauchfuss, T. B.; Ruffing, C. J.; Fultz, W. C.; Rheingold, A. L. *J. Am. Chem. Soc.* **1984**, *106*, 5379.

(32) Ou, C.-C.; Miskowski, V. M.; Lalancette, R. A.; Potenza, J. A.; Schugar, H. J. *Inorg. Chem.* **1976**, *15*, 3157.

(33) Stynes, H. C.; Ibers, J. A. *Inorg. Chem.* **1971**, *10*, 2304.

at 2.435 Å, the S atom is slightly displaced from collinearity with the Ru–N(3) bond axis [S–Ru–N(3) = 172.4°, S–Ru–N(4) = 84.1°], and the tilt angle Ru–S–X (see crystal structures section), which describes the angle formed between the C–S–C bisector and the Ru–S bond axis, is 139.4°. Furthermore, the S–C bond length in the complex is calculated at 1.842 Å, slightly larger than its value in the free ligand [1.805 Å calculated, 1.805 (2) Å experimentally[29]], and the C–S–C angle also opens slightly from 100.7° in the free ligand [experimental value[29] 99.05 (4)°] to 104.8° in the complex. Inspection of Tables V and VI shows that most of these structural parameters are in very close agreement with those determined from X-ray crystallography or electron diffraction. The differences between calculated and observed Ru–S and Ru–S–X parameters will be discussed later. The peculiar coordination geometry and small distortions in the structure of the thioether ligand can be rationalized from a detailed analysis of the electronic wave functions and orbital energies.

The analysis begins with a brief examination of the thioether electronic ground state ($^1A_1$, $C_{2v}$ symmetry, $z$ axis as $C_2$ axis, $xz$ as the C–S–C plane). The three highest lying MOs emerging from the ab initio calculations have orbital energies of −8.97, −11.71, and −13.44 eV, respectively. Assuming the validity of Koopmans' theorem,[24] these MO energies correlate well with the three lower energy features appearing in the photoelectron spectrum at 8.65, 11.2, and 12.6 eV, respectively.[22] Amplitude contour plots of these orbitals are shown in Figure 4. The highest occupied MO (HOMO = −8.97 eV)) is a $\pi$-type lone-pair orbital located almost exclusively on S (>90%) as a $3p_y$ atomic orbital [$S(\pi)$, $b_1$ symmetry, Figure 4a]. The next highest MO (−11.71 eV) is a $\sigma$-type orbital which may be viewed as the in-phase combination of the two S–C $\sigma$-bond orbitals [$S(\sigma)$, $a_1$ symmetry, Figure 4b]. It has substantial (58%) S $3p_z$ character but the sulfur 3s character is very limited (8%), since the 3s orbital acts like a localized core orbital positioned below −20 eV. The corelike nature of this orbital has been noted previously in studies of Cu(II)–thioether bonding.[34] It would thus be incorrect to consider this orbital as a conventional in-plane, $sp^2$-type hybrid lone pair on S. The third MO (−13.44 eV) is then the out-of-plane combination of the two $\sigma$-bond orbitals [$b_2$ symmetry, Figure 4c], which on S involves the $3p_x$ orbital (26%) but no 3s character due to symmetry restrictions. There is a gap of ca. 2 eV between this orbital and the next occupied MOs, the C–H bond orbitals. Consequently, only the thioether HOMO appears to be an orbital capable of significant interaction with the Ru(III) center since it is the only high-lying orbital heavily concentrated on S. The two $\sigma$-type orbitals appear suitable mainly for secondary interactions, with the $S(\sigma)$ orbital being the better of the two for both energetic and electron density reasons.

Imagine next the thioether ligand approaching a square-pyramidal $Ru(NH_3)_5^{3+}$ fragment from the direction of the open coordination site. A sterically most favorable approach will clearly occur when the S atom is collinear with the Ru–N(3) bond axis and the $CH_3$ groups are directed outward with the C atoms staying in the plane determined by the Ru, S, N(1), N(3), and N(5) atoms (7). This orientation appears to give rise to favorable $p(\pi)$–$d(\pi)$

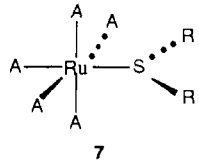


7

interaction between the thioether $S(\pi)$ HOMO and the Ru $4d_{xy}$ orbital; the latter orbital is, however, already partially occupied with one electron. Furthermore, there will be only minor $\sigma$-type interaction along the Ru–S axis due to the energetic mismatch between the thioether donor $S(\sigma)$ MO and the most likely acceptor orbital, the Ru $4d_{x^2-y^2}$ orbital, as well as the absence of strong directionality toward Ru in the $S(\sigma)$ electron density. In fact, geometry optimization with such maximum collinearity and coplanarity imposed leads to a large Ru–S bond length (ca. 2.55 Å), indicating that only weak electronic interactions are possible in this orientation.

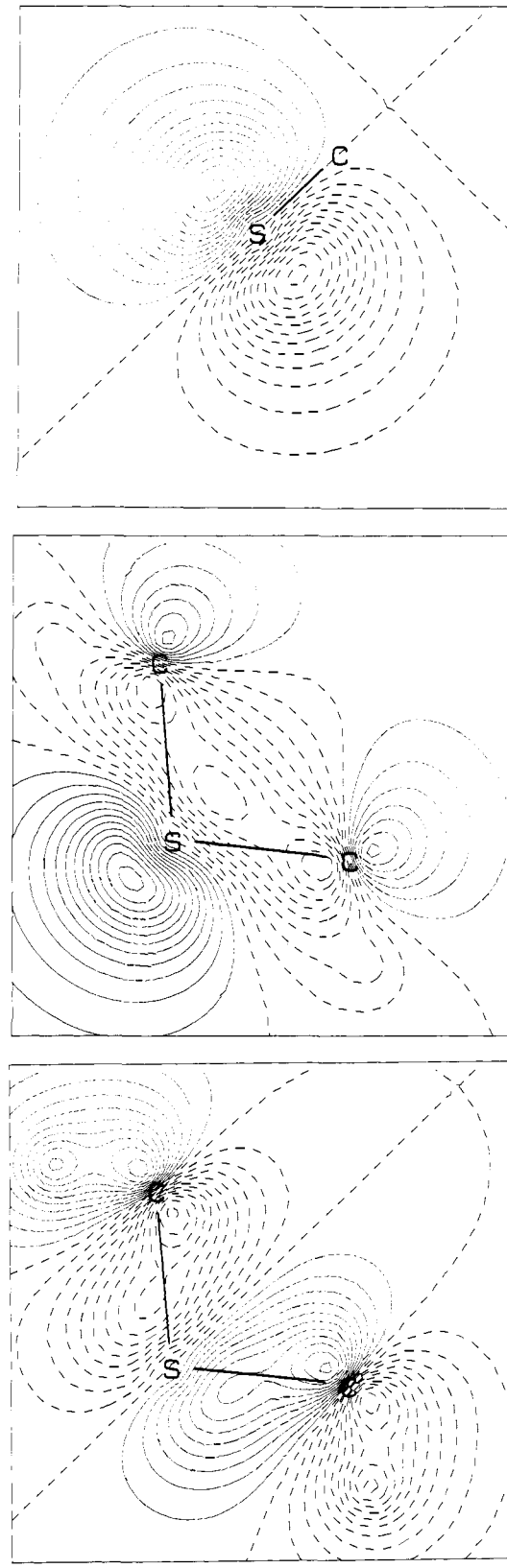


**Figure 4.** Amplitude contour plots of the three highest-lying occupied molecular orbitals in $S(CH_3)_2$. Heavy (dashed) lines indicate positive (negative) amplitude values. (a, top) The HOMO, $S(\pi)$, orbital plotted in the symmetry plane ($yz$) perpendicular to the $SC_2$ plane ($xz$). (b, middle) The symmetric combination of S–C bond orbitals, $S(\sigma)$, plotted in the $xz$ plane. (c, bottom) The antisymmetric combination of S–C bond orbitals plotted in the $xz$ plane.

(34) Penfield, K. W.; Gewirth, A. A.; Solomon, E. I. *J. Am. Chem. Soc.* **1985**, *107*, 4519.

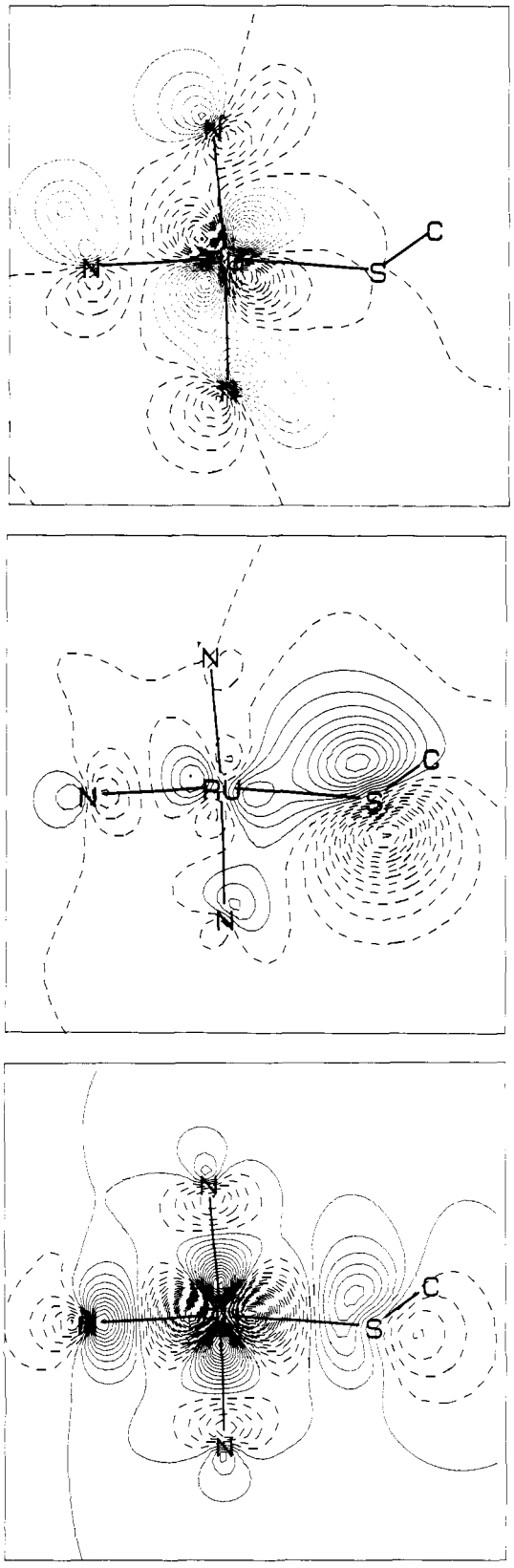


**Figure 5.** Amplitude contour plots of the frontier molecular orbitals in $[(NH_3)_5Ru^{III}S(CH_3)_2]^{3+}$. Heavy (dashed) lines indicate positive (negative) amplitude values. (a, top) The singly occupied orbital, $4d_{xy}$, plotted in the *xy* symmetry plane. (b, middle) The highest lying, doubly occupied MO in the complex plotted in the *xy* plane. This orbital corresponds to $S(\pi)$ in free dimethyl thioether (Figure 4a). (c, bottom) The lowest lying, unoccupied orbital in the complex ($4d_{x^2-y^2}$).

It is therefore important to get a direct $\sigma$-type interaction between the good donor and acceptor orbitals available, i.e., between the $S(\pi)$ and Ru $4d_{x^2-y^2}$ orbitals. This is accomplished by

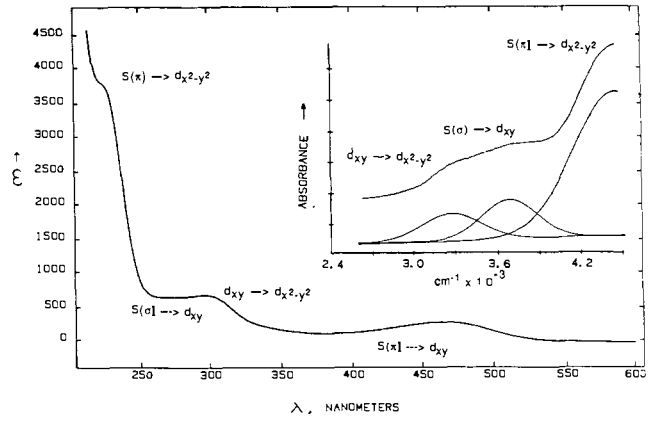


**Figure 6.** UV-vis spectrum of a $4.3 \times 10^{-4}$ M solution of **1** in $CH_3OH/H_2O$ (50/50, v/v) at 298 K. The inset shows the UV spectrum of the same mixture at 77 K, and Gaussian deconvolution into three absorptions is noted.

tilting the C–S–C plane relative to the Ru–N(1)–N(3)–N(5) plane (**5**), thus reorienting the $S(\pi)$ orbital away from the $d_{xy}$ orbital toward $d_{x^2-y^2}$. The destruction of local symmetry around S permits orbital mixing and facilitates rehybridization around this atom which may further increase the $\sigma$-type component in the electronic Ru–S interaction. Finally, pushing the S atom away from collinearity with Ru–N(3) toward N(4) also enhances the interaction with the $4d_{x^2-y^2}$ acceptor orbital. The amplitude contour plots in Figure 5 show that the singly occupied MO in the complex is a virtually unperturbed Ru $d_{xy}$ orbital (Figure 5a). There may be signs of a very small interaction having occurred between the $d_{xy}$ orbital and the thioether $S(\sigma)$ orbital but there are no signs of $d_{xy}$–$S(\pi)$ interaction. The plot of the rehybridized $S(\pi)$ orbital as it appears in the complex (Figure 5b) does show mixing with the Ru orbitals, however. The stabilizing interaction is primarily with the $d_{x^2-y^2}$ orbital and is perhaps most readily seen in the plot of $d_{x^2-y^2}$, the lowest unoccupied MO (LUMO) in the complex (Figure 5c). It has clearly mixed with $S(\pi)$ in an antibonding fashion, thus implying that the doubly occupied $S(\pi)$ orbital has mixed in $4d_{x^2-y^2}$ character in a bonding fashion. The contours around S are oriented differently normal to the thioether plane in Figure 5b and c, however, indicating that the $S(\sigma)$ orbital also plays a role in the interaction with $d_{x^2-y^2}$. Even with the extended basis sets employed for Ru and S in our calculations, it appears that the strength of the $\sigma$ interaction still is underestimated and as a result the computed Ru–S bond length is 0.05 Å too long and the tilt angle (Ru–S–X) too large, perhaps by 15° (Table VI).[35] The rehybridization and electron donation from the thioether unit to Ru weaken the S–C bonds, which lengthen by ca. 0.035 Å in the complex, and open the C–S–C angle by ca. 4°.

The electronic population analysis on the complex indicates that the Ru atom carries a positive charge of 0.90e or, equivalently, the formally triply charged ion has received 2.10e from the ligands. The donation amounts to 0.43e from the $S(CH_3)_2$ unit and 0.33e on the average from each $NH_3$ unit. Further breakdown of the calculated populations shows that the S atom donates only 0.07e and that the $CH_3$ groups each provide 0.18e (0.07e from C, 0.11e from the H atoms). On Ru, the charge is accepted primarily into the $4d_{x^2-y^2}$ (0.81e), the $4d_{z^2}$ (0.70e), and the 5s orbitals (0.46e). The population in the formally singly occupied $4d_{xy}$ orbital is only 1.06e, in accordance with the minimal thioether–$d(\pi)$ interaction noted above.

**Electronic Spectroscopic Results.** The solution spectra for $[A_5RuS(CH_3)_2]^{3+}$ reported by Stein and Taube include features at 22 100 $cm^{-1}$ (453 nm, $\epsilon$ = 300), 35 100 $cm^{-1}$ (285 nm, $\epsilon$ = 930), and 45 500 $cm^{-1}$ (220 nm, $\epsilon$ ca. 5000).[36] The lowest energy

(35) It should be noted that the estimated value for the Ru–S–X angle in **3** is 133.3°, only 6.1° less than the calculated value.
(36) Stein, C. Y.; Taube, H. *Inorg. Chem.* **1979**, *18*, 1168.

absorption was assigned as a ligand to metal charge-transfer (LMCT) band. Our solution spectra of **3** (not shown) agree overall with those of Taube and Stein but the broad feature from ca. 250 to 350 nm appears to contain at least two distinct electronic transitions. The THT complex **1** exhibits solution spectra at room temperature (Figure 6) that are similar to those of **3**. At low temperature, the broad absorption at ca. 300 nm in the solution spectrum is partially resolved (Figure 6, inset). Gaussian deconvolution of the low-temperature spectrum is consistent with the presence of two absorptions at 32 700 $cm^{-1}$ (306 nm) and 36 900 $cm^{-1}$ (271 nm) flanked by a more intense, higher energy absorption at 44 700 $cm^{-1}$ (224 nm). Thus, there appear to be four transitions belonging to a $(NH_3)_5Ru^{III}$–thioether complex between 20 000 and 50 000 $cm^{-1}$.

The thioether ligand should be optically silent in solution below 40 000 $cm^{-1}$. In dimethyl thioether, the lowest energy absorption features observed in the gas phase near 44 000 $cm^{-1}$ have been assigned to the first member of a Rydberg series [$S(\pi) \rightarrow 4s$].[37] A higher energy band near 49 000 $cm^{-1}$ is probably a valence shell excitation [$S(\pi) \rightarrow \sigma^*$].[38] Our semiempirical INDO calculations on free dimethyl thioether predict two valence-type transitions [$S(\pi) \rightarrow \sigma^*$ type] at 42 300 and 46 100 $cm^{-1}$. For tetrahydrothiophene, we calculate analogous transitions at 42 300 $cm^{-1}$ (oscillator strength $f = 0.011$) and 45 200 $cm^{-1}$ ($f < 10^{-3}$). The "parent" $Ru(NH_3)_6^{3+}$ complex shows numerous weak, overlapping absorptions to doublet and quartet states between 20 000 and 50 000 $cm^{-1}$ arising from excitations out of the $t_{2g}^5$ ground-state configuration; a more prominent feature around 36 400 $cm^{-1}$ ($\epsilon$ ca. 500) probably contains some charge-transfer type character.[39] As described previously, our calculations on the "parent" hexammine complex show no spin-allowed transitions below 31 000 $cm^{-1}$ and the spin-allowed d–d transitions in the 31 000–45 000-$cm^{-1}$ range all have very small oscillator strengths ($f < 10^{-4}$).[2] Thus, certainly both the weak, low-energy (ca. 22 000 $cm^{-1}$) and strong, high-energy (ca. 45 000 $cm^{-1}$) bands observed in the Ru–thioether complex must be indicative of metal–ligand interactions.

The ground state of **1** is still appropriately described as $^2A'$ ($^2d_{xy}$), although **1** only has the *xy* plane as an approximate symmetry plane. Only transitions polarized in this plane are calculated with appreciable intensities ($f > 10^{-3}$). The lowest energy transition[40] is calculated at 23 600 $cm^{-1}$ ($f = 0.020$) and is exclusively $S(\pi) \rightarrow d_{xy}$ in character, i.e., LMCT from the rehybridized ligand HOMO to the singly occupied metal d orbital. The computed and observed weakness of this transition is supportive of the bonding interpretation given above, which involves very little overlap between the $S(\pi)$ and $d_{xy}$ orbitals. In the 30 000–40 000-$cm^{-1}$ range, two electronic transitions with intensity are calculated at 35 300 and 37 300 $cm^{-1}$, respectively. The former is a metal d–d transition ($d_{xy} \rightarrow d_{x^2-y^2}$, $f = 0.005$) and the latter transition is predominantly $S(\sigma) \rightarrow d_{xy}$ LMCT in character ($f = 0.018$). The weakness of this LMCT transition underscores the minimal overlap between the two orbitals involved. Excitations to these two electronic states are responsible for the broad absorption in the 270-nm range. At still higher energy, we calculate several weak metal d–d transitions in the range 42 000–44 500 $cm^{-1}$ ($f \sim 0.002$). These states are not observed as a separate spectral feature since we also calculate a far more intense transition at 47 000 $cm^{-1}$ ($f = 0.089$). The assignment for this transition is $S(\pi) \rightarrow d_{x^2-y^2}$ LMCT, i.e., formally an excitation from the thioether HOMO to one of the Ru(III) $e_g^*$ set of orbitals. Its pronounced intensity (calculated as well as observed) is also in complete accordance with the claim that direct $\sigma$-type interaction and at least moderately good overlap occur between these orbitals. Also, it demonstrates that even though the octahedral crystal field splitting parameter ($\Delta_0$) is approximately 36 000 $cm^{-1}$ for $Ru(NH_3)_6^{3+}$,[3] thus causing electronic transitions to the $e_g^*$ set in typical $A_5Ru^{III}X$ systems to be beyond the usual quartz UV spectral range, this is no longer the case when a weaker field ligand replaces one ammonia molecule at a long coordination distance and with a peculiar orientation. A partial vacancy has been created in the coordination sphere and therefore the $\sigma$-type d orbital pointing in that direction ($d_{x^2-y^2}$) is not destabilized nearly as much as its partner in the $e_g^*$ set ($d_{z^2}$). Consequently, with a high-lying donor orbital present, transitions to this metal orbital may appear within the normal UV range, albeit still at high energy. There are no further transitions calculated below 51 000 $cm^{-1}$, at which point the $N(\sigma) \rightarrow d_{xy}$ LMCT transitions begin to appear. The electronic transitions, intensities, and assignments for **1** are summarized in Table VII.

**Table VII.** Experimental and Calculated Transition Energies ($cm^{-1}$) and Intensities in **1**

| exptl[a] | $\epsilon$ | calcd | $f$ | assignt |
|---|---|---|---|---|
| 22 000 | 250 | 23 600 | 0.020 | $S(\pi) \rightarrow d_{xy}$ |
| 32 700 | 400 | 35 300 | 0.005 | $d_{xy} \rightarrow d_{x^2-y^2}$ |
| 36 900 | 530 | 37 300 | 0.018 | $S(\sigma) \rightarrow d_{xy}$ |
| 44 700 | 4300 | 47 000 | 0.089 | $S(\pi) \rightarrow d_{x^2-y^2}$ |

[a] At 298 K; see caption of Figure 6.

It is worthwhile to point out that a thioether ligation arrangement involving maximum collinearity and coplanarity with the $A_5Ru$ system, i.e., **7**, is incompatible with the experimentally observed spectra. Such an arrangement with dominant $S(\pi)$–$d(\pi)$ interaction should lead to a strong, low-energy absorption band [$S(\pi) \rightarrow d_{xy}$] and weak, high-energy bands arising perhaps from the $S(\sigma) \rightarrow d_{xy}$ and $S(\pi) \rightarrow d_{x^2-y^2}$ excitations. The latter transitions would involve negligible overlap between the donor and acceptor orbitals. The intensities of the LMCT transitions in these complexes are critically dependent on the value of the Ru–S–X tilt angle. The orientation and bonding pattern described for **5** is, of course, fully compatible with the observed UV spectra.

## Concluding Remarks

The studies reported here have probed the structural, electronic, and spectroscopic features of Ru(III)–thioether bonding. The low oscillator strength of the thioether–Ru(III) LMCT absorption may now be understood as a consequence of the orientation of the thioether donor (HOMO) and Ru(III) acceptor ($d_{xy}$) orbitals. A second consequence of the poor thioether–Ru(III) overlap is that the thioether ligand exerts an unexpectedly small ligand field. Thus, the Ru $d(\sigma^*)$ orbital ($d_{x^2-y^2}$) that has a lobe pointed toward the S atom is lowered in energy, becomes accessible spectroscopically, and allows $S(\pi) \rightarrow$ Ru $d(\sigma^*)$ LMCT to be observed at the relatively low energy of 45 000 $cm^{-1}$. The relative orientation of the $S(\pi)$ and Ru $d_{x^2-y^2}$ orbitals in **1** is analogous to the orientation of the $S(\pi)$ and Cu $d_{x^2-y^2}$ orbitals in **6**. Therefore, the intensities of the LMCT bands involving these orbitals would be expected to be similar,[41] although their energies are quite different.

The structural and electronic-structural peculiarities of Ru(III)–thioether bonding were not available for the theoretical study of intervalence electron transfer between Ru–S chromophores separated by oligospirocyclobutane spacers.[12] Clearly, accurate estimates of the electronic coupling between these mixed-valence chromophores require detailed knowledge of the metal–ligand interactions as well as the orbital nature of the hydrocarbon spacer.[42] Our results emphasize the fact that metal–thioether structure and electronic structure are not readily deduced from simple geometric and valence considerations. In particular, the dominant influence of the spatially and energetically suitable $S(\pi)$ thioether orbital for bonding must be stressed.

(37) Scott, J. D.; Causley, G. C.; Russell, B. R. *J. Chem. Phys.* **1973**, *59*, 6577.

(38) Robin, M. B. *Higher Excited States of Polyatomic Molecules*; Academic Press: New York, 1975; Vol. I, II.

(39) Navon, G.; Sutin, N. *Inorg. Chem.* **1974**, *13*, 2159.

(40) There are two low-lying states calculated near 1000 $cm^{-1}$ above the ground state. These states correspond to alternative occupancies of the five d electrons within the quasidegenerate $t_{2g}$ set.

(41) Dagdigian, J. V.; McKee, V.; Reed, C. A. *Inorg. Chem.* **1982**, *21*, 1332.

(42) Rendell, A. P. L.; Bacskay, G. B.; Hush, N. S. *J. Am. Chem. Soc.* **1988**, *110*, 8343.

**Acknowledgment.** The research of H.J.S. and J.A.P. was supported in part by the National Science Foundation (Grant CHE 84-17548), the National Institutes of Health (Grant GM-37994), and the David and Johanna Busch Foundation. The diffractometer–crystallographic computing facility at Rutgers was purchased with NIH Grant 1510 RRO 1486 O1A1. The research of K.K.-J. was supported by the National Institutes of Health (Grant GM-34111) and the donors of the Petroleum Research Fund, administered by the American Chemical Society. Generous grants of computer time from the IBM Corp., the John von Neumann Supercomputer Center, and the New Jersey Commission on Science and Technology are gratefully acknowledged. We thank Profs. S. S. Isied and H. B. Gray for helpful discussions and advice, Dr. J. T. Blair for installing the population analysis routines in our GAMESS program, and the Engelhard Corp. for a generous sample of $RuCl_3 \cdot 6H_2O$.

**Supplementary Material Available:** Tables of hydrogen atom parameters and anisotropic thermal parameters for **1–3** (7 pages); listings of observed and calculated structure factors for **1–3** (78 pages). Ordering information is given on any current masthead page.

# Synthesis, Characterization, and Electrical Response of Phosphazene Polyelectrolytes

**S. Ganapathiappan, Kaimin Chen, and D. F. Shriver***

*Contribution from the Department of Chemistry and Materials Research Center, Northwestern University, Evanston, Illinois 60208.* *Received September 12, 1988*

**Abstract:** New phosphazene-based polymers have been synthesized, which function as single-ion conductors of either sodium or halide ions. As a prelude to the synthesis of these polymers, similar substitution reactions were carried out on hexchlorocyclotriphosphazene and the products were well characterized. The polyelectrolytes were characterized by $^1H$ NMR, $^{31}P$ NMR, IR, DSC, and ac complex impedance studies. The temperature dependence of the conductivity of these polyelectrolytes follows the VTF equation, indicating that, as with polymer–salt complexes, ion transport is promoted by polymer-segment motion. The ionic conductivity of the polyelectrolytes containing bromide and iodide is 2 orders of magnitude higher than that of the sodium polyelectrolytes at 30–80 °C.

There has been considerable interest in the mechanism of charge transport in polymer and polyelectrolytes and in the potential applications of these materials in solid-state devices.[1-4] Phosphazene- and siloxane-based comb polymers have been reported to exhibit high conductivity with alkali metal salts of trifluoromethanesulfonates, thiocyanates, and iodides.[5-7] The drawback with these polymer–salt complexes as polymer electrolytes is that both cations and anions are mobile, and as a result, fundamental studies of single-ion transport are difficult. In addition, most applications of these materials are based on the transport of only one ion, such as $Li^+$ in a lithium battery. In these applications the mobility of the anion leads to unwanted gradients in electrolyte concentration. A solution to this problem is to covalently attach the counterion to the polymer backbone. In the absence of solvent, conventional polyelectrolytes are rigid solids, which show poor conductivity. The introduction of plasticizers into polyelectrolytes greatly increases their conductivity, but plasticized systems are inherently less stable than pure polymers.[8] Recently, polyelectrolytes of crosslinked phosphates[9] and poly[(oligo(oxyethylene)methacrylate)-*co*-(alkali-metal methacrylates)][10] have been shown to be sodium ion conductors but show poor conductivity at room temperature.

We report the synthesis of elastomeric phosphazene polyelectrolytes in which the side groups are short chain oligo ether alkoxy and alkoxy sulfonate, quaternary or trialkylammonium salts. These new polyelectrolytes exhibit good ionic conductivity without added plasticizers or inorganic salts. A preliminary communication has appeared.[11]

## Experimental Section

**Materials.** All the experimental manipulations were carried out under an inert atmosphere of dry nitrogen. Tetrahydrofuran (THF) was distilled under nitrogen from sodium benzophenone ketyl. Acetonitrile (MeCN) was distilled from calcium hydride. The sodium salt of 2-hydroxyethanesulfonic acid, 15-crown-5, and sodium spheres (Aldrich) were used as received; 2-(2-methoxyethoxy)ethanol (MeeOH) (Aldrich) was dried over molecular sieves (4A) and distilled before used. Poly(ethylene glycol methyl ether) (PEGOH) of average molecular weight 350, *N,N*-dimethylethanolamine and *N,N*-diethylethanolamine (Aldrich) were dried over molecular sieves (4A) before used. All haloalkanes were distilled prior to use, and other chemicals were reagent-grade purity.

Dialysis tubes (American Scientific Products) used in the purification of the polymer normally had a cutoff molecular weight of 1000, but a molecular weight cutoff of 3500 was used for polymers synthesized with the sodium salt of PEGOH.

Sodium ethane sulfonate was prepared by the neutralization of ethanesulfonic acid with sodium hydroxide in an aqueous solution and was recrystallized from methanol. Reactions involving iodoalkanes were carried out in the dark. Poly(dichlorophosphazene), $(NPCl_2)_n$ (**1**) was prepared by the thermal polymerization of hexachlorocyclo-

(1) Tonge, J. S.; Shriver, D. F. *Polymers for Electronic Applications*; Lai, J., Ed.; CRC: Boca Raton, FL, in press.
(2) Ratner, M. A.; Shriver, D. F. *Chem. Rev.* **1988**, *88*, 109.
(3) See for example: *Polymer Electrolyte Reveiws*; MacCallum, J. R., Vincent, C. A., Eds.; Elsevier Applied Science: New York, 1987; Chapters 1–3.
(4) Armand, M. B. *Annu. Rev. Mater. Sci.* **1986**, *16*, 245.
(5) Blonsky, P. M.; Shriver, D. F.; Austin, P.; Allcock, H. R. *J. Am. Chem. Soc.* **1984**, *106*, 6854.
(6) Blonsky, P. M.; Shriver, D. F.; Austin, P. E.; Allcock, H. R. *Solid State Ionics* **1986**, *18/19*, 258.
(7) Spindler, R.; Shriver, D. F. *Macromolecules* **1988**, *21*, 648.
(8) Hardy, L. C.; Shriver, D. F. *J. Am. Chem. Soc.* **1985**, *107*, 3823.
(9) LeNest, J. F.; Gandini, A.; Cheradame, H.; Cohen-Addad, J. P. *Polym. Commun.* **1987**, *28*, 302.
(10) (a) Tsuchida, E.; Kobayashi, N.; Ohno, H. *Macromolecules* **1988**, *21*, 96. (b) Kobayashi, N.; Hamada, T.; Ohno, H.; Tsuchida, E. *Polym. J.* **1986**, *18*, 661.
(11) Ganapathiappan, S.; Chen, K.; Shriver, D. F. *Macromolecules* **1988**, *21*, 2299.

0002-7863/89/1511-4091$01.50/0 